Ceramics International **23** (1997) 483–488

PII: S0272-8842(96)00058-2
0272-8842/97 $17.00+.00

Wear Simulation of Si_3N_4 Cutting Tool Material on a Pin-On-Disc Tester

Xingzhong Zhao, Jiajun Liu, Baoliang Zhu, Hezhou Miao & Zhenbi Luo

Tribology Research Institute, Tsinghua University, Beijing 100084, China

(Received 2 May 1996; accepted 27 June 1996)

Abstract: Si_3N_4-based ceramic cutting tools are used nowadays for machining cast iron, nickel-based alloys, etc. Austenitic stainless steel AISI 321 is one of the most difficult to cut materials. In order to investigate the wear behaviour of Si_3N_4 ceramic when cutting the stainless steel, wear tests are carried out on a pin-on-disc tribometer, which can simulate a realistic cutting process. The selected load range is from 58.8 N to 235.2 N, the speed range is from 0.8 m/s to 3.2 m/s. The test results show that the wear of Si_3N_4 ceramic increases with both load and speed and the wear of the ceramic is mainly caused by adhesion between the rubbing surfaces. Scanning electron microscope (SEM), electron probe microanalyser (EPMA) and energy dispersive X-ray analyser (EDXS) were used for examinations of the worn surfaces. The wear mechanisms of Si_3N_4 ceramic sliding against the stainless steel were discussed in detail. © 1997 Elsevier Science Limited and Techna S.r.l.

1 INTRODUCTION

During the last 20 years, Si_3N_4-based ceramics have been increasingly used as wear resistant materials. One of the most important applications of these materials is for cutting tools, which are applied nowadays in machining cast iron and nickel-based alloys.[1–4] Their performance on steels, however, are known to be less than satisfactory.[5] The wear rate of a silicon nitride cutting tool is two orders of magnitude higher when maching AISI 1045 steel than when machining grey cast iron.[6] The high cratering wear of sialon ceramics when machining AISI 1045 steel is caused by the chemical dissolution of sialon grains, followed by pull-out of sialon grains from the glassy intergranular phase.[7]

Austenitic stainless steels are one of the most widely used class of materials and they are very different from carbon steel in many properties. However, little knowledge about the wear behaviour of Si_3N_4-based ceramics is available when they are used for cutting austenitic stainless steels. The objectives of this study are to investigate the wear behaviour of a Si_3N_4-based ceramic on a pin-on-disc tribometer under dry conditions. Compared with real machining tests, pin-on-disc tests are simple, quick, and their conditions of solicitation may be widely varied and well controlled, they seem to be appropriate tests for tool life simulation. Some work has been done in wear mechanism analysis of ceramic tool materials and the comparison of wear data from pin-on-disc tests and cutting behaviour of ceramics.[8,9] In this test, the worn surfaces of the Si_3N_4 ceramic were examined and analysed by using scanning electron microscope (SEM), electron probe microanalyser (EPMA), energy dispersive X-ray analyser (EDXA), and X-ray photoelectron spectroscopy (XPS).

2 EXPERIMENTAL PROCEDURE

2.1 Test machine and specimens

Wear tests are carried out on a pin-on-disc tribometer. The pin specimen is fixed, the disc specimen, driven by a motor, can rotate at different speeds. The schematic diagram of the tester is shown in Fig. 1. Initial line contact is formed

between the pin and the disc, which can simulate well the contact form of a cutting tool and workpiece in a realistic cutting practice. The pin is made from hot-pressed Si_3N_4 ceramic, having a size of 5×5×25 mm; the disc was machined from AISI 321 stainless steel, 56 mm in diameter and 6 mm in thickness. The frictional surface roughness of the pin and the disc is $Ra = 0.32\ \mu m$ and $Ra = 0.21\ \mu m$, respectively. Some properties of the Si_3N_4 ceramic are listed in Table 1.

2.2 Test method

Friction and wear tests are operated under dry conditions. The room temperature is about 20°C. The sliding speeds between the rubbing surfaces are from 0.8 m/s to 3.2 m/s, the selected load range is from 58.8 N to 235.2 N. Each pair had a 30 min running time under selected speed and load and at least two tests were performed. Before and after testing, the specimens were ultrasonically cleaned in an acetone bath for 15 min.

The wear scar width of the pin is measured under a photo microscope, then the volume and wear rate can be calculated. The friction force is transmitted by a transducer to a recorder continuously during the test, from which the friction coefficient can be obtained. The worn surfaces are examined by using scanning electron microscopy (SEM), energy dispersive X-ray spectroscopy analyser (EDXS), electron probe microanalyser (EPMA), and X-ray photoelectron spectroscopy (XPS). During XPS analysis, an Al kα line was used, the pass energy was 35.75 eV, and the binding energy C1s (284.6 eV) was used as reference.

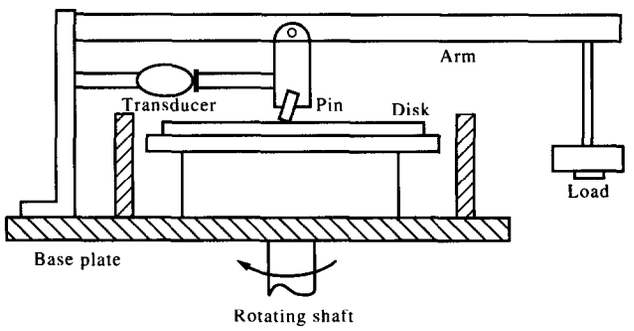

Fig. 1. The schematic diagram of the tester.

Table 1. The physical and mechanical properties of the Si_3N_4 ceramic

Properties	Unit	Value
Amount	wt%	>80
Density	$g.cm^{-3}$	3.5
Hardness	Hv	1900
Bending strength	MPa	750
Elastic modulus	GPa	290
Fracture toughness	$MPa.m^{1/2}$	6.3
Grain size	μm	<1.3
Impurities		TiC, Al_2O_3

3 RESULTS AND DISCUSSION

3.1 Effects of load on friction coefficient and wear rate

Figures 2 and 3 show the variation of friction coefficient and wear rate with load, respectively. It can be seen from the figures that the friction coefficient and wear rate of the ceramic increase with load. SEM examinations found that stainless steel was transferred on the worn ceramic surfaces at both low and high loads. The rapid increase of the wear rate at higher load (235.2 N) may be caused by severe adhesion between the rubbing surfaces and the increase of the microfracture of the ceramic, which was confirmed by the SEM examinations of the worn Si_3N_4 ceramic surface and the wear debris [see Fig. 4(a) and (b) (the arrow in Fig. 4(a) points to the microfracture pit) and Fig. 5 (microfracture fragments)]. The EDXS spectrum of point A in Fig. 5 is shown in Fig. 6, the element compositions indicate that the particle came from

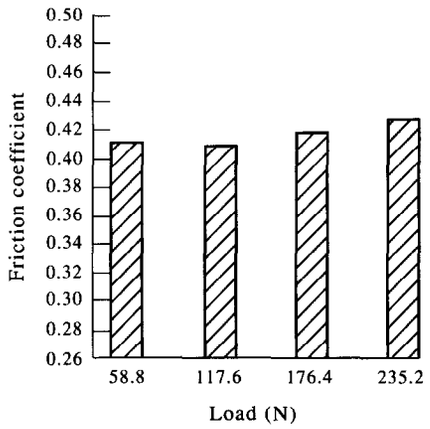

Fig. 2. Variation of friction coefficient with load.

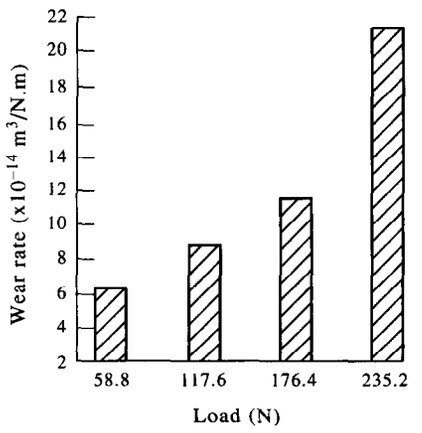

Fig. 3. Variation of wear rate of the ceramic with load.

Si_3N_4 ceramic. For comparison, the SEM morphology of the worn Si_3N_4 surface of lower load is shown in Fig. 7.

3.2 Effects of speed on friction coefficient and wear rate

The variations of friction coefficient and wear rate with speed are shown in Figs 8 and 9. Similar to the effects of load, the friction coefficient and wear rate increase with speed. However, the friction coefficient increases more rapidly and reaches a much higher value compared with the effect of load. High speed brings about a large amount of friction heat, which will aggravate the adhesion between the rubbing surfaces, so both the friction coefficient and wear rate increase with speed. In general, the SEM morphologies of the worn Si_3N_4 surfaces obtained at different speeds are similar to Figs 4 and 7 (stainless steel transfer on the worn

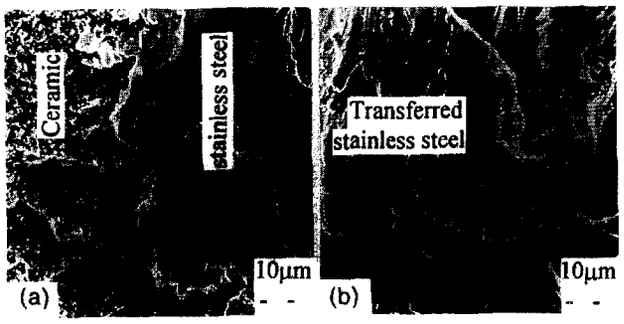

Fig. 4. SEM morphologies of the worn ceramic surfaces (dry, 235.2 N, 1.6 m/s).

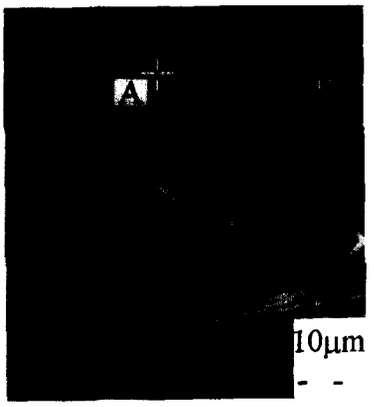

Fig. 5. SEM examination of the wear debris (dry, 235.2 N, 1.6 m/s).

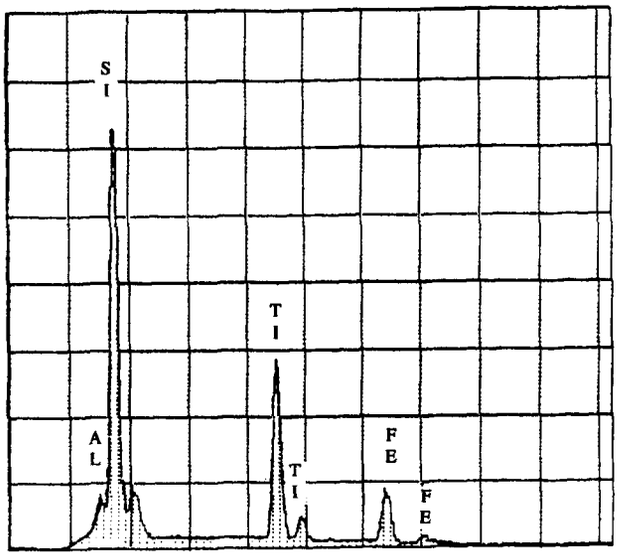

Fig. 6. EDXA spectrum of the point A in Fig. 5.

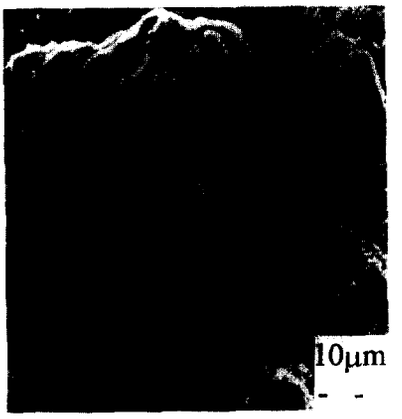

Fig. 7. SEM morphology of the worn ceramic surface (dry, 117.6 N, 1.6 m/s).

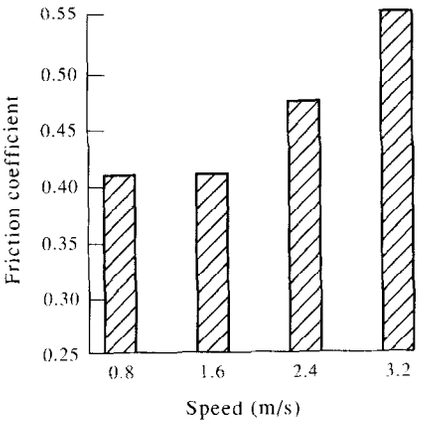

Fig. 8. Variation of friction coefficient with speed.

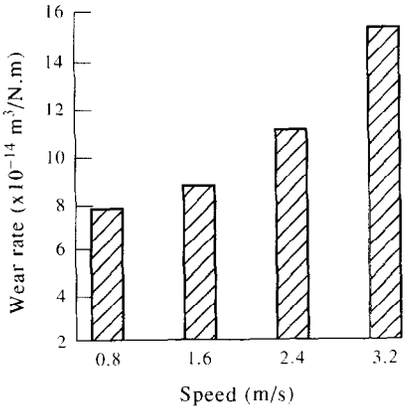

Fig. 9. Variation of wear rate of the ceramic with speed.

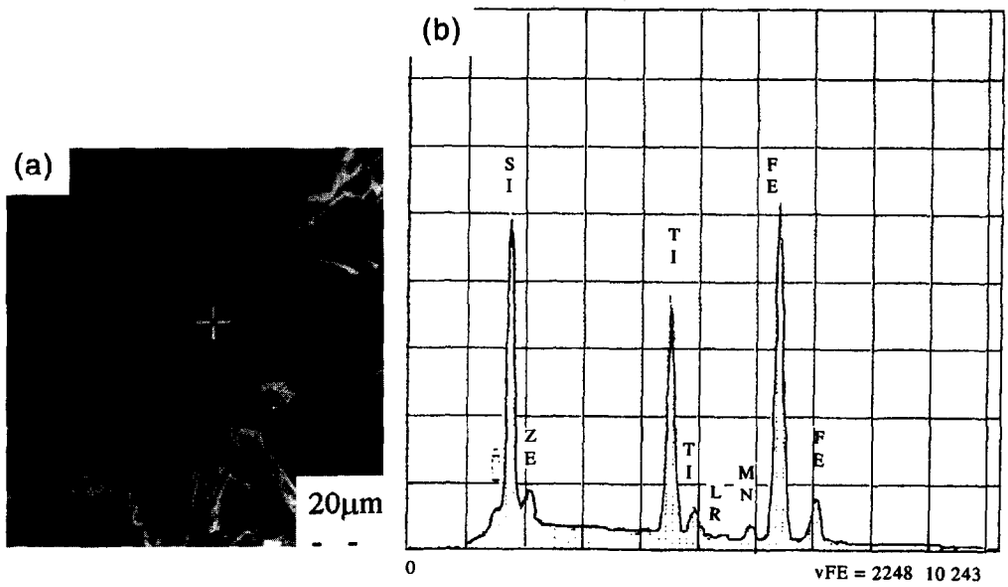

Fig. 10. (a) SEM morphology of the wear debris (dry, 117.6 N, 1.6 m/s). (b) EDXA spectrum of the marked point in (a).

ceramic surfaces also occurs at different speeds), but at high speed (3.2 m/s in this test), it can be found that some ceramic grains melt on the worn ceramic surfaces (see Section 3.4 for details).

3.3 Wear mechanisms of Si_3N_4 ceramic

It can be seen from Figs 4 and 7 that stainless steel transfers on the ceramic surfaces because of adhesion between the rubbing surfaces. It can also be found by comparing Figs 4 and 7 that the amount of the transferred stainless steel increases with load, and many larger transferred stainless steel flats formed on the worn ceramic surface at higher load (235.2 N), while only smaller stainless steel flats formed at lower load (117.6 N).

From the SEM examinations, it is not difficult to deduce the wear process of the ceramic. There is a high chemical affinity between iron and silicon nitride,[10,11] and strong adhesion will ocurr when Si_3N_4 and stainless steel are put into sliding contact. With the relative movement of the rubbing surfaces, the adhesion junctions will be torn off, resulting in the transfer of stainless steel on the rubbing ceramic surface (the adhesive points or areas will be broken more frequently in stainless steel surface because of its relatively low shear strength).

The transferred stainless steel on the ceramic surface will be subjected to shear and compressive stresses repeatedly with the rubbing movement, which will cause microcracks and microfractures in the ceramic surface or its subsurface. Meanwhile, the transferred stainless steel is also subjected to adhesive force coming from the rubbing stainless steel surface, which will peel off the transferred stainless steel flats. Ceramic microfracture pieces or Si_3N_4 grains will also be peeled off or pull-out and quit the ceramic surface with the peeled off stainless steel flats, which gives rise to the wear of the ceramic.

The adhesion–peeling off mechanism of the ceramic wear can be confirmed by the EDXS analysis result of the wear debris [see Fig. 10(a) and (b)]. The intense Si peak in Fig. 10(b) shows the wear debris is not only the stainless steel, it is combined particles of Si_3N_4 and stainless steel (caused by adhesion). It is clear in Fig. 11 that the stainless steel wear piece contains the ceramic particles (the arrow points to the ceramic particles which are embedded in a stainless steel piece).

3.4 Chemical wear and element diffusion

In addition to the adhesion–peeling off mechanism meantioned above, the wear of the ceramic is also attributed to chemical wear–oxidation of the Si_3N_4 grains and the element interdiffusion between the rubbing surfaces. XPS spectrum of the worn

Fig. 11. SEM examinations of the wear debris (dry, 117.6 N, 1.6 m/s).

ceramic surface shows that SiO_2 was produced on the worn surface, the binding energy of Si_2p was 103.3 eV (see Fig. 12). EPMA examinations found some microballs on the worn Si_3N_4 surfaces [see Fig. 12(a)]. Composition distribution analyses corresponding to Fig. 12(a) are shown in Fig. 12(b)–(d), which indicate that the microballs come from ceramic grains and stainless steel, respectively. Si_3N_4 grains may be oxidized to produce SiO_2 at high temperature (caused by high speed), then the SiO_2 grains, TiC grains (contained in the ceramic) and some stainless steel debris were molten under the severe frictional conditions to form the microballs. Although SiO_2 and TiC have high melting points, the ceramic grains could still melt due to the following factors. First, the ceramic is not composed of only Si_3N_4 or TiC, it contains a lot of additives, such as Al_2O_3, CaO and Y_2O_3, which would reduce the melting points of the SiO_2 and TiC grains. Second, the heat conductivity of the ceramic is rather low. Third, large amounts of deformation heat and friction heat will be produced in the rubbing process because of the very high toughness of the stainless steel and the relatively low heat conductivity (compared with carbon steel). Fourth, as the small contact area of the ceramic sample maintains contact state throughout the whole rubbing process, the temperature of its contact surface could be much higher than that of

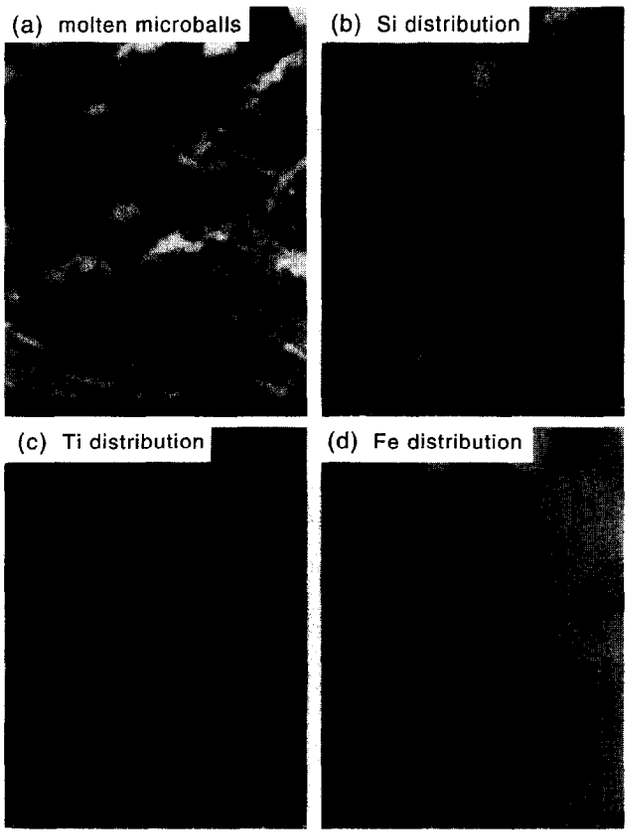

Fig. 12. EPMA examinations of the worn ceramic surfaces (dry, 117.6 N, 3.2 m/s).

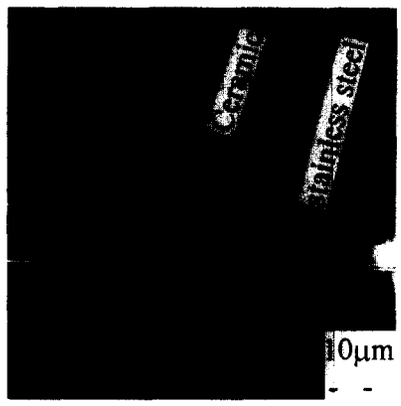

Fig. 13. Element Si diffusion in stainless steel.

the stainless steel surface. All these factors result in very high temperatures on the rubbing surfaces, especially on the rubbing ceramic surface, which causes the ceramic grains to melt. Moreover, according to Ref. 8, the chemical dissolution of Si_3N_4 grains in wear chip should be more severe considering that the stainless steel has higher toughness and lower heat conductivity than AISI 1045 steel, which also accelerates the melting of the ceramic grains.

The EDXS analysis of the cross-section of the worn ceramic surface showed that element diffusion occurs between the worn ceramic surface and the transferred stainless steel flats (see Fig. 13). The Si element diffusion in stainless steel will also result in the structural destruction and strength decrease of the ceramic surface, which will accelerate the wear of the ceramic.

Adhesion, melting and element diffusion are not isolated, they are relative to each other. With load and speed increasing, real contact area and friction heat increase, which will accelerate the melting of the ceramic grains and element diffusion, resulting in heavy adhesive wear.

4 CONCLUSIONS

From the above test results and surface examinations, the following conclusions can be summarized.

1. In Si_3N_4 ceramic/stainless steel sliding contacts, the wear of the ceramic is mainly caused by the adhesion–peeling off process. Stainless steel firstly transfers on to the ceramic surface, then the transferred stainless steel flats will be subjected to repeated shear and compressive stresses untill they are peeled off the rubbing ceramic surface. When the transferred stainless steel flats are peeled off the ceramic surface, some ceramic fragments or grains are also pulled out and taken away.

2. The wear of the ceramic is also attributed to the oxidation of Si_3N_4 grains and the Si element diffusion in the stainless steel. The element diffusion destroys the microstructure of the ceramic surface and decreases its strength. Moreover, element interdiffusion will aggravate the adhesion between the rubbing surfaces, and then result in more severe adhesive wear of the ceramic.
3. With load and speed increasing, the friction heat of the rubbing surfaces increase rapidly, which will accelerate the oxidation of the ceramic grains, element diffusion and adhesion between the rubbing surfaces, so the wear of the ceramic increases with load and speed. In addition, higher load also brings about more severe microfracture wear of the ceramic.

ACKNOWLEDGEMENTS

The authors would like to thank National Natural Sciences Foundation of China and Laboratory of Solid Lubrication, Lanzhou Institute of Chemical Physics, Chinese Academy of Sciences, for their financial support to this project.

REFERENCES

1. BLACKMAN, T. N., *Foundryman*, **3** (1990) 17–24.
2. AUCOTE, J. & FOSTER, S. R., *Mater. Sci. Technol.*, **2** (1986) 700–708.
3. RICHARDS, N. & ASPINWALL, D., *Int. J. Machine Tools Manufact.*, **29** (1989) 575–588.
4. SAMANTA, S. K., SUBRAMANIAN, K. & EXIS, A., US Patent No. 4323325.
5. ASIBU, E. K., *J. Manufact. Syst.*, **9** (1990) 159–168.
6. BRUN, M. K. & LEE, M., *Ceram. Eng. Sci. Proc.*, **4** (1983) 646–662.
7. RIGAUT, R., CHEN, Y. M. & SAINT CHELY, J., *Lubr. Eng.*, **50** (1994) 485–489.
8. BRANT, G., GERENDAS, A. & MIKUS, M., *J. Eur. Ceram. Soc.*, **6** (1990) 273–290.
9. TONSHOFF, H. K., WOBKER, H. G. & BRANDT, D., *Lubr. Eng.*, **50** (1995) 163–168.
10. KRAMER, B. M. & SUH, N. P., *J. Eng. Ind.*, **102** (1980) 303–309.
11. KRAMER, B. M. & JUDD, P. K., *J. Vac. Sci. Technol.*, **A3** (1985) 2439–2444.